LAWRENCE
LIVERMORE
NATIONAL
LABORATORY

UCRL-CONF-155673

Development of a Process Model for CO_2 Laser Mitigation of Damage Growth in Fused Silica

M.D. Feit, A.M. Rubenchik, C.D. Boley, and M.D. Rotter

November 1, 2003

SPIE Boulder Damage Symposium XXXV-Annual Symposium on Optical Materials for High Power Lasers
Boulder, Colorado
September 22-24, 2003

Updated October 14, 2003

Development of a Process Model for CO_2 Laser Mitigation of Damage Growth in Fused Silica

M.D. Feit*, A.M. Rubenchik, C.D. Boley, M. Rotter

University of California
Lawrence Livermore National Laboratory
P.O. Box 808 L-491
Livermore, CA 94550

Abstract

A numerical model of CO_2 laser mitigation of damage growth in fused silica has been constructed that accounts for laser energy absorption, heat conduction, radiation transport, evaporation of fused silica and thermally induced stresses. This model will be used to understand scaling issues and effects of pulse and beam shapes on material removal, temperatures reached and stresses generated. Initial calculations show good agreement of simulated and measured material removal. The model has also been applied to LG-770 glass as a prototype red blocker material.

Introduction

The possibility of using CO2 laser treatment both to remove damaged material from and to anneal the resulting silica surface was suggested some time ago[1,2,3,4.] . However, it has only been in recent years that more systematic investigation[5] indicated that laser damage growth in fused silica, problematic because of transverse damage site size grows exponentially[6] with the number of laser shots, could be mitigated by this method. Currently, considerable effort is being made to find optimal conditions for this type of mitigation[7] on a NIF relevant scale. As part of this effort, we are developing a detailed numerical model of the laser absorption, material removal and stress generation caused by such mitigation. This is an expansion of the semi-analytic model[8] developed earlier.

The advantages of possessing such a model are to aid optimization of the mitigation process with respect to controllable beam parameters such as power, beamshape, and exposure time. Here we report on the verification and first results obtained using this model.

Approach

We investigated various approaches to implementation of a process model. In the end, we combined an in-house thermal code (THALES) with a commercial code (ANSYS) for thermal induced stresses. Commercial codes such as ANSYS and COSMOS have the advantages of treating many physical phenomena, and well developed user interfaces. They also have the disadvantage of treating many physical phenomena since this results in a steep learning curve before they can be used productively. A further disadvantage is the impossibility of making modifications to such codes. Writing our own code has the advantages of knowing precisely what is included in the numerical model and being relatively easy to modify, but the large disadvantage that, having to start from scratch, it would be a long time before any useful results would be obtained. We avoided this disadvantage by modifying the THALES code written by Charles Boley, originally to model drilling[9] with copper vapor lasers and later applied to beam dump studies and interactions of the solid state heat capacity laser with various materials. The necessary modifications made included thermal diffusion in cylindrical symmetry (r-z), temperature dependent conductivity to treat losses due to radiation transport, and calculation of evaporation.

* Correspondence: email feit1@llnl.gov, telephone 925-422-4128, fax 925-422-5718

Two simplifying assumptions make the simulations tractable. The first is that surface deformation is neglected in the thermal calculation, i.e. the evaporative flux is calculated for the original surface and integrated over time to give the amount of material removed. This is a good assumption for shallow spots (much wider than deep). The second assumption is that the spot is cylindrically symmetric. This is mainly to reduce required computation time. We anticipate that in future simulations of crack healing, full 3D calculations will be carried out. The models have been benchmarked by comparison with both analytic solutions and available experimental results. Both of these codes are well tested and the approximations and assumptions made are known.

In trying to understand the implications of nonconstant stress distributions, it is useful to divide the stress into two parts – the average and the deviatoric. The average stress is just the average of the principal stress components. It is a scalar and corresponds to a uniform pressure. The deviatoric stress is the difference between the full stress and the average and is principally responsible for plastic deformation and fracture. We will present typical results in terms of the deviatoric stresses.

Results

Some of the initial mitigation studies done at LLNL used a 50 μs pulsed CO2 laser (Gaussian pulse shape) with a flattop beam shape produced by aperturing the beam. We estimated the heating and stress generation for such conditions. Series of 1,3 and 10 shot mitigation craters were formed at several fluences. A typical experimental result[10] for hole depth, measured interferometrically, is shown in Fig. (1). The mean depth of a patch inside the mitigated 10 shot spot was 32 μm indicating an evaporation depth of 3.2 μm per shot. There is good linearity in depth with number of shots as shown in Fig. (2). This is consistent with a simple back of the envelope estimate (see Appendix A) of 2-4 μm / shot. The good agreement of the simple estimate is somewhat fortuitous, but the general agreement in order of magnitude is convincing since evaporation rate depends exponentially on temperature.

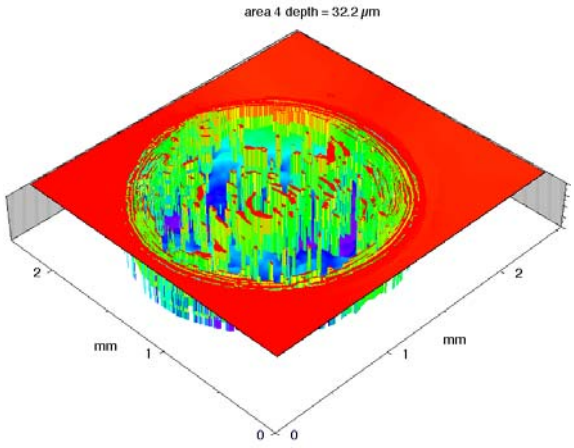

Fig. 1: Depth profile for 10 shots at 28 J/cm^2. Some data points are missing and have arbitrarily been set to zero in the image and in processing.

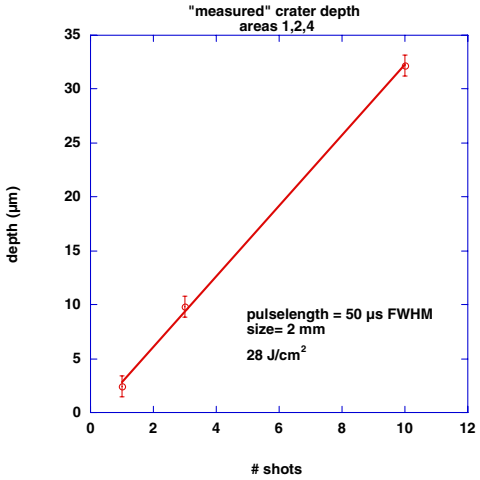

Fig. 2: Experimental depth of crater as a function of number of shots.

The detailed numerical calculations for the top-hat beam shape and Gaussian pulse shape give the temperature distribution shown in Fig. (3). Note that the surface temperature is determined by absorption, evaporative cooling and heat conduction. The numerical value of about 3500 °C is comparable to the back of the envelope value of about 3700-4000 °C

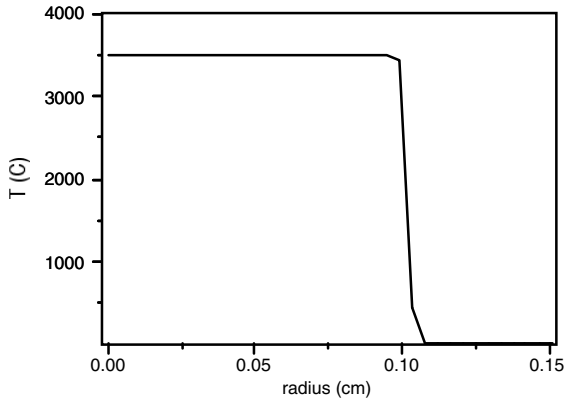

Fig. 3a: Surface temperature toward end of pulse for 28 J/cm^2 50 µs pulse.

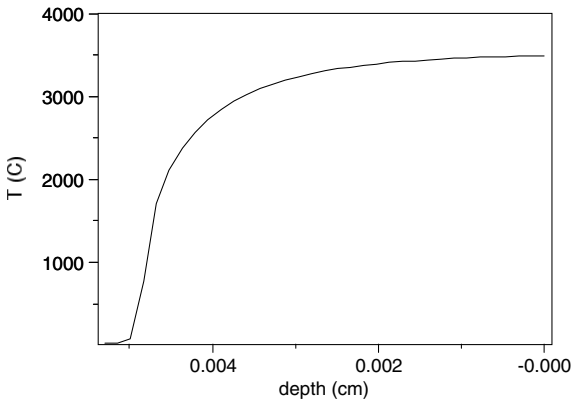

Fig. 3b: Longitudinal temperture variation corresponding to Fig. 3a. High temperatures extend 40 µm into silica. The thermal diffusion length is 14 µm.

Evaporative losses are calculated as a function of time as shown in Fig. (4). The simulation predicts a loss of 4 µm/shot in comparison to the experimental value of 3.2 µm/shot.

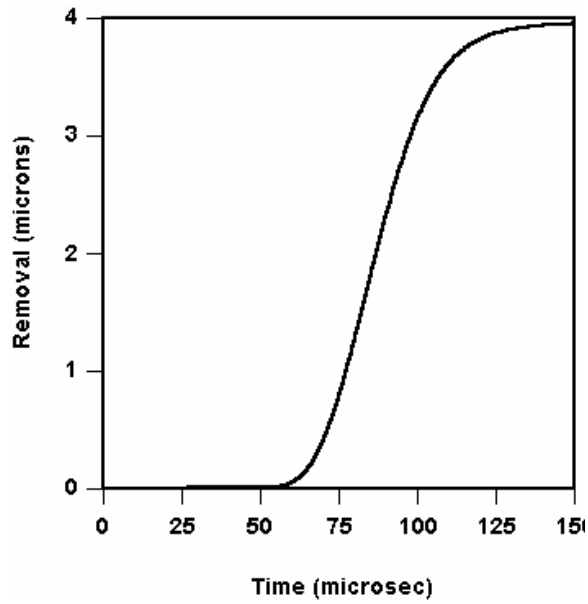

Fig. 4: Calculated material removal via evaporation for 50 µs pulse. Center of pulse is at time 85 µs.

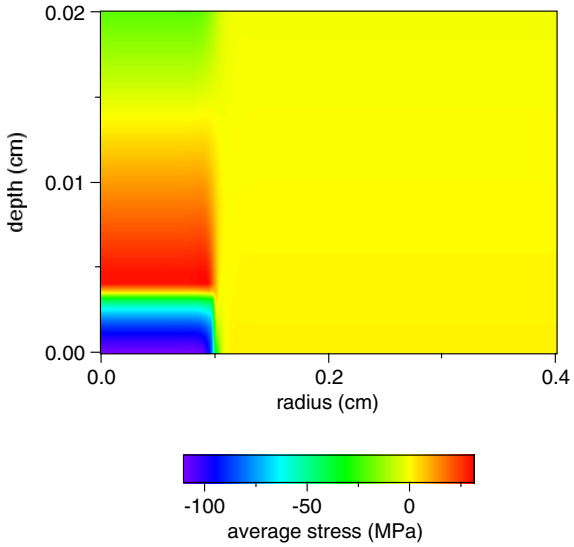

Fig. 5: Calculated average stress, which corresponds to hydrostatic pressure. Compression over 100 MPa occurs in surface layer.

Since we do not have direct measurements of the induced stress to compare to, we validated the stress calculation portion of the model by evaluating thermally induced stresses in two simple situations for which analytic solutions are known. These are the cases of plane strain in a cylinder and a sphere with a Gaussian temperature distribution. The analytic and numerical results are presented in Appendix B. The numerical simulation results were virtually indistinguishable from the analytic solutions. This gives us confidence in the numerical model.

Typically, the stress distribution extends far outside the region in which the temperature varies significantly. Since a boundary condition (typically assumption of a free surface) must be imposed at the outside of the simulated region, and the boundary condition significantly modifies the solution near the outer boundary, this means the simulation boundary has to be sufficiently far away from the region in which laser energy is absorbed. The nature of this difference is illustrated in Appendix C which compares the hoop stress induced for a spherical region of constant temperature embedded in either an infinite medium or a finite medium. The stress at the outer boundary of the finite region differs by a factor of 3 from that of the infinite medium. However, since the stress typically drops with the cube of distance, the stress in the vicinity of the heated region can be calculated accurately by having the outer boundary far enough away.

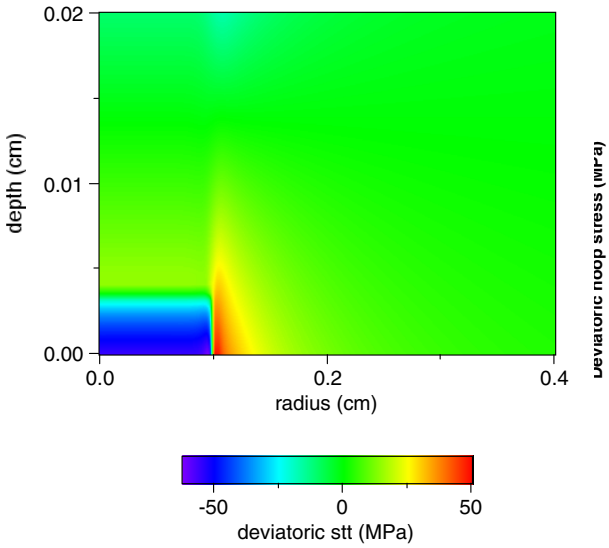

Fig. 6: Deviatoric hoop stress. Note that stress over 50 MPa occurs just outside the beam shadow where the material is cool.

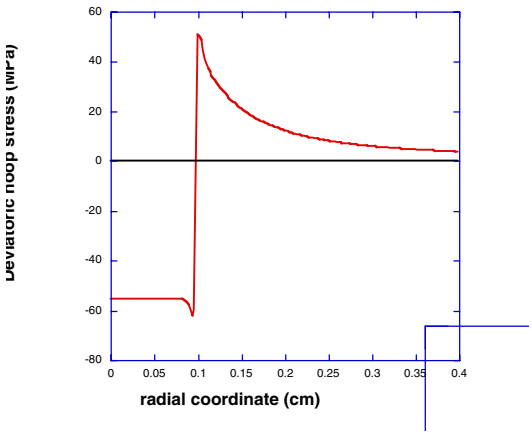

Fig. 7: Deviatoric hoop stress at surface. Highest stress is just outside heated region.

The average stress (i.e. average of principal components) at pulse end corresponding to the same conditions as Fig. (4) is shown in Fig. (5). Compressive stress is indicated by negative values, tensile stress by positive. The values at the upper boundary (farthest distance from the surface at which laser energy is absorbed) are affected by the boundary condition as noted above. Strong compressive stresses exist near the surface.

It is more interesting to look at the deviatoric hoop stress shown in Fig. (6). A lineout of the stress at the surface is shown in Fig. (7). The important point here is that while compressive stress still occurs in the

central heated region (compare Fig.(3a)), large tensile hoop stresses occur just outside this region. The magnitude of this stress, 50 MPa, is near the strength of the material.

Note that large mitigated sites will have stress distributions extending further along the surface. Since large sites may be expected to have larger pre-existent cracks, more susceptible to crack growth, this could be a problem. This is especially true in the case shown here where the largest hoop stresses occur in cold, i.e. brittle, material. Further simulations and experiments not shown here indicate that a graded beam shape, e.g. Gaussian, can alleviate this problem by reducing thermal gradients and allowing some warming of material outside the region of removal.

Summary

We have constructed a process model for CO2 laser mitigation of surface damage growth in fused silica that accounts for laser energy absorption, heat conduction and (approximately) radiation transport. The model includes material removal by evaporation and thermally induced stresses. Simulated values for material removal are in good agreement with experiment. This is a sensitive test since evaporation rates depend exponentially on temperature. Larger damage sites are expected to be more difficult to mitigate as they lead to higher susceptibility to fracture. Both beam and pulseshapes may be modified to allow material removal while minimizing susceptibility to fracture.

Acknowledgement

This work was performed under the auspices of the U.S. Department of Energy by
University of California Lawrence Livermore National Laboratory under contract No. W-7405-Eng-48.

Appendix A: Simple estimate of material removal by evaporation

The vaporization rate v can be treated as an activated process, i.e.

$$v = v_0 \exp(-U/kT)$$

where the activation energy U is 3.6 eV. The thickness d of material removed is given by
$d = \int v\, dt$. Now, by energy balance, if L is the energy/volume used in evaporation, then
$Lv = \alpha_e I$
where α_e is the fraction of incident light absorbed and I is the laser intensity. This expression assumes the material is not heated. A better version would be
$v(L + \rho C \Delta T) = \alpha_e I$
where ρ=is the density and C is the specific heat. Depending on whether or not the material is dissociated, L should be just the energy of evaporation, about 13 KJ/cm^3 or that of evaporation plus dissociation, about 30 KJ/cm^3. For a flat in time pulse of 50 μs, and laser fluence of 28 J/cm^2, solving the above equation then gives
T = 4066°K and d=6.6 μm for L=30 KJ/cm^3 or
T = 4324°K and d=12.1 μm for L=13 KJ/cm^3.
Finally, we note that for a Gaussian pulseshape, assuming the temperature follows the laser intensity, we have to integrate over the pulseshape. This gives estimates of 1.97 and 3.76 μm, respectively, for the two values of L. Thus, our simple estimate is that for fluence of 28 J/cm^2 and a 50μs Gaussian pulse, about 2-4 μm of fused silica will be evaporated.

Appendix: B: Benchmarking stress calculations

1. Temperature induced plane strain in cylindrical symmetry

Consider the cylindrical temperature distribution

$$T(r) = T_m r^2 / b^2$$

in a cylinder of radius b. The induced radial, hoop and longitudinal stresses are given by[11]

$$\sigma_r = \frac{\alpha E T_m}{4(1-\nu)}\left(1-\rho^2\right)$$

$$\sigma_\theta = \frac{\alpha E T_m}{4(1-\nu)}\left(1-3\rho^2\right)$$

$$\sigma_z = \frac{\alpha E T_m}{2(1-\nu)}\left(\nu-2\rho^2\right)$$

where E is Young's modulus, ν is the Poisson ratio, α the coefficient of thermal expansion and ρ=r/b. . The stresses calculated for this case with ANSYS agree extremely well with the analytic solution as shown in Fig.(A1).

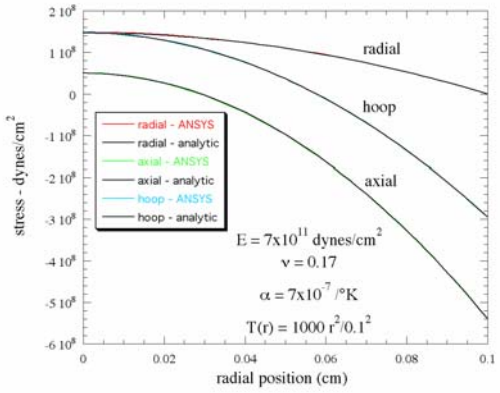

Figl A1: Comparison of stresses calculated with ANSYS with analytic solution for radial, hoop and longitudinal stresses. Analytic and numerical curves lie on top of each other. Physical properties usef are for fused silica.

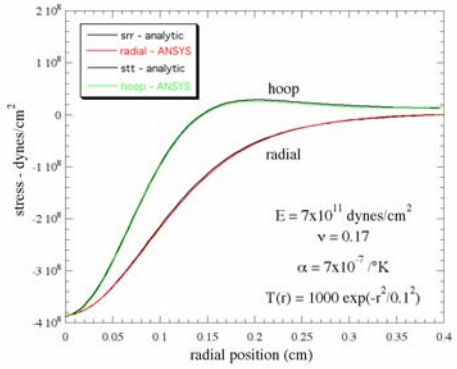

Fig. A2: Comparison of analytic and simulated stresses for Gaussian temperature distribution inside sphere. Again the analytic and numerical curves lie on top of each other.

As a second example, more realistic in that the temperature drops with radius, consider a sphere of radius b win which the temperature has a Gaussian distribution:

$$T(r,z) = T_m \exp\left[-\left(r^2+z^2\right)/b^2\right]$$

or

$$T(\rho) = T_m \exp\left[-\rho^2/b^2\right]$$

Here r is the cylindrical radius and □ the spherical radius. The exact solution for stress in this case is[11]

$$\sigma_r = \frac{2\alpha E}{(1-\nu)}\left[u(\rho_m) - u(\rho)\right]$$

$$\sigma_\theta = \frac{\alpha E}{(1-\nu)}\left[u(\rho) + 2u(\rho_m) - T(\rho)\right]$$

where

$$u(\rho) \equiv \frac{1}{\rho^3}\int_0^\rho T(\rho)\rho^2 d\rho \quad = \quad \frac{T_m}{4\rho^3}\left[\sqrt{\pi}\,\mathrm{Erf}(\rho) - 2\rho e^{-\rho^2}\right]$$

A comparison of simulated and analytic stresses is given in Fig. A2. The spatial distribution of radial stress is shown in Fig. A3.

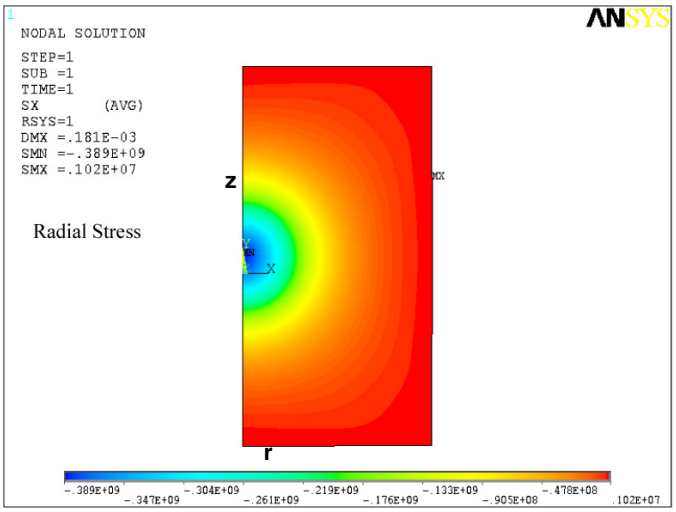

Fig. A3: Distribution of radial stress (dyne/cm2) as function of radius (x-axis)
And depth (y-axis) for spherical benchmark case.

Appendix C: Boundary conditions for stress calculation

The numerical calculation of stress must have a boundary condition at the largest radius on the numerical mesh. The commercial code treats this as a free surface. This is a crucial point because the stress distribution extends much farther into the material than the temperature distribution and the free surface condition can lead to much different results than that for a medium of infinite transverse size. This can be illustrated by a simple analytic situation.

Consider a spherical region of constant temperature T0 and radius b embedded inside a sphere of radius R. The hoop stress for this case can be found by the methods given in ref.[11] as

$$\sigma_{\theta\theta} = \frac{\alpha E T_0}{1-\nu}\left(\left(\frac{b}{r}\right)^3 + 2\left(\frac{b}{R}\right)^3\right)$$

The point to note is that for an infinite medium, the stress at r=R is only 1/3 of that at the same point for a finite medium of outer radius R. Thus, the two solutions always differ significantly at r=R. However, if R is sufficiently large, the $1/R^3$ behavior dies out rapidly away from the outer boundary. Thus, in the raster

plots of stress given here, the stress values at maximum radius should be discounted, but the distribution nearer to the center is reliable.

References

[1] P. A. Temple, D. Milam and W. H. Lowdermilk, "CO2 laser polishing of fused silica surfaces for increased laser damage resistance at 1.06 μm",Nat. Bur. Stand. (U.S.) *Spec. Publ*. **568,** 229-36 (1979).

[2] P. A. Temple and M. J. Soileau," 1.06 nm laser-induced breakdown of CO2-laser-polished fused SiO2", Nat. Bur. Stand. (U.S.) *Spec. Publ*. **620**, 180-89 (1981).

[3] P.A. Temple, W.H. Lowdermilk, D. Milam, "Carbon dioxide laser polishing of fused silica surfaces for increased laser-damage resistance at 1064 nm", *Appl. Opt*. **21**, 3249-55 (1982).

[4] P. A. Temple, S. C. Seitel, and D. L. Gate," CO2 Laser Polishing of Fused Silica: Recent Progress", Nat. Bur. Stand. (U.S.) *Spec. Publ*. **669**, 130-37 (1984)

[5] L.W.Hrubesh, M.A.Norton, W.A.Molander, E.E.Donohue, S.M.Maricle, B.M.Penetrante, R.M.Brusasco, W.Grundler, J.A.Butler, J.W.Carr, R.M.Hill, L.J.Summers, M.D.Feit, A.Rubenchik, M.H.Key, P.J.Wegner, A.K.Burnham, L.A. Hackel and M.R.Kozlowski, "Methods for mitigating surface damage growth on NIF final optics", *Laser-Induced Damage in Optical Materials: 2001*, Proc. SPIE **4679**, (2002).

[6] M.A. Norton, L.W. Hrubesh, Z. Wu, E.E. Donohue, M.D. Feit, M.R. Kozlowski, D. Milam, K.P. Neeb, W.A. Molander, A.M. Rubenchik, W.D.f Sell and P. Wegner, "Growth of laser initiated damage in fused silica at 351 nm", *Laser-Induced Damage in Optical Materials: 2000* , Proc. SPIE 4347**,**. 468-468 (2001).

[7] R.R. Prasad, "Enhanced optical damage resistance of large 3ω optics using XeF and CO_2 lasers", *Laser Induced Damage in Optical Materials:* 2003, Proc. SPIE **5273** (2004) (paper 5273-49 in these proceedings)

[8] M.D. Feit and A.M. Rubenchik, ""Mechanisms of CO2 laser mitigation of laser damage growth in fused silica", *Laser Induced Damage in Optical Materials:2002*, Proc. SPIE **4932**, 91-102 (2003)

[9] C. D. Boley and J. T. Early, "Computational Model of Drilling with High Radiance Pulsed Lasers," Proc. Intern. Conf. on Applications of Lasers and Electro-Optics, Orlando, FL, Vol. **79,** p. 499 (1994).

[10] The actual experimental data contains an overall tilt which has been removed as well as an arbirary zero of height. We have attempted to put the zero of height in the flat portion of the surface outside the mitigated spot. Note that not all the data sets have perfectly flat outer regions.

[11] B.A. Boley and J.H. Weiner, *Theory of Thermal Stresses*, J.H. Wiley & Sons, (1960)